24th COBEM - 2017

24th ABCM International Congress of Mechanical Engineering
December 3-8, 2017, Curitiba, PR, Brazil

COBEM-2017-1029
AN EFFICIENT SELECTIVE MODAL H$_\infty$ CONTROL FOR MECHANICAL STRUCTURES

Helói F. G. Genari
Academic Department of Electronics, Federal University of Technology - Paraná, Curitiba, Brazil
e-mail:heloigenari@utfpr.edu.br

Eurípedes G. O. Nóbrega
Pablo S. Meirelles
Department of Computational Mechanics, University of Campinas, Campinas, Brazil
e-mails:egon@fem.unicamp.br and pablo@fem.unicamp.br

Abstract. *This paper explores the modal H_∞ methodology for active vibration control of real flexible structures. The modal technique has been recently proposed by this research group, associating modal and robust control concepts by means of the new modal H_∞ norm. This norm allows an appropriate control energy distribution in each mode using an H_∞ controller, which leads to a high modal selectivity, an adequate overall performance, and robustness. The modal technique effectiveness is investigated in a cantilever aluminum beam with non-collocated piezoelectric transducers and is compared with the regular H_∞ control methodology. Theoretical and experimental results show that the modal H_∞ control provides a significant performance gain over the regular H_∞ strategy.*

Keywords: *Active vibration control, modal control, modal H_∞ control, H_∞ control, spillover.*

1. INTRODUCTION

The increasing demand of high structural performance has conducted to the development of ever larger, lighter, and more flexible structures. These structures are usually subjected to disturbance that may lead to undesired vibrations if an efficient vibration control algorithm is not applied properly (Genari *et al.*, 2015; Mechbal and Nóbrega, 2015; Pereira and Serpa, 2015). In consequence, the active vibration control technique development has been receiving a relevant attention in the last decades (Hu and Ng, 2005; Halim, 2004; Mechbal and Nóbrega, 2012), considering that active approaches usually provide better performance than semi-active and passive methods (Preumont, 2011).

The infinite number of structure vibration modes may be considered the main challenge in the controller design for real mechanical structures. Usually, the control techniques are developed for a finite number of vibration modes, which may lead the control system to instability due to the excitation of neglected dynamics, a phenomenon known as spillover (Balas, 1979; Meirovitch *et al.*, 1983; Genari *et al.*, 2017c). The localization of sensors and actuators may also render a more complex structure dynamics to control because most structures are non-collocated, which means they may have zeros on the right half-plane (Gosiewski and Kulesza, 2013; Mastory and Chalhoub, 2014). The H_∞ control approach is able to deal with spillover and non-collocated structures, using weighing filters to avoid the excitation of the neglected dynamics (Serpa and Nobrega, 2005). However, filters limit the controller actuation in contiguous low-frequency bands, preventing mode selectivity in terms of both the amplitude and the frequency (Genari *et al.*, 2017b). On the other hand, modal control methods are able to control each vibration mode, however, these methods are very sensitive to the spillover phenomenon (Baz and Poh, 1990; Inman, 2001; Cinquemani *et al.*, 2015).

Recently, our research group proposed a methodology to merge the modal and the H_∞ control features (Genari *et al.*, 2017a), aiming to achieve higher global vibration reduction by means of mode selectivity. This is possible due to the modal H_∞ norm, which weights each mode according to the desired structure behavior. The modal controller is obtained by the minimization of the modal H_∞ norm, using an equivalent problem formulation that can be solved by adopting a well-known procedure for the regular H_∞ control problem. However, this technique still requires further experimental results to test the performance effectiveness. Therefore, this paper examines experimentally the modal H_∞ control for disturbance rejection in a flexible structure, aiming to extend the experimental results present in (Genari *et al.*, 2017a). The structure is a cantilever aluminum beam with non-collocated piezoelectric transducers. Initially, a regular H_∞ controller is designed, whose performance is used as reference. Then, some modal H_∞ controllers are designed with different modal weights in order to show the mode selectivity. Experimental results show that using the modal H_∞ approach may increase the global vibration reduction compared to the regular H_∞ strategy.

2. STATE-SPACE MODAL MODEL

The modal robust control technique is configured to use the state-space models in the modal canonic form. Therefore, a brief description of this model representation is presented in this section. A generic flexible structure with multiple transducers can be modeled by the following second-order differential pair of equations:

$$\begin{aligned}&\mathbf{M}\ddot{\mathbf{p}}(t) + \mathbf{D}\dot{\mathbf{p}}(t) + \mathbf{K}\mathbf{p}(t) = \mathbf{B_w}\mathbf{w}(t) + \mathbf{B_u}\mathbf{u}(t) \\ &\mathbf{y}(t) = \mathbf{C_d}\mathbf{p}(t) + \mathbf{C_v}\dot{\mathbf{p}}(t) + \mathbf{C_w}\mathbf{w}(t) + \mathbf{C_u}\mathbf{u}(t),\end{aligned} \tag{1}$$

in which $\mathbf{M}$ is the mass matrix, $\mathbf{D}$ is the damping matrix, $\mathbf{K}$ is the stiffness matrix, and $\mathbf{B_w}$ and $\mathbf{B_u}$ are the respective input matrices. The signal $\mathbf{p}(t)$ denotes the displacements, $\mathbf{w}(t)$ represents the disturbance forces acting on the structure, $\mathbf{u}(t)$ represents the control forces, and $\mathbf{y}(t)$ are the measured output signals modeled through the output matrices $\mathbf{C_d}$, $\mathbf{C_v}$, $\mathbf{C_w}$, and $\mathbf{C_u}$. In general, a reduced order model is used to represent a frequency band of interest, in which a modal matrix is used to obtain the manageable model. Considering the number of vibration modes is m, the modal matrix is defined as

$$\mathbf{\Phi} = \begin{bmatrix} \phi_\mathbf{1} & \phi_\mathbf{2} & \dots & \phi_\mathbf{m} \end{bmatrix}.$$

Using the coordinate transformation $\mathbf{p}(t) = \mathbf{\Phi}\mathbf{q}(t)$ and pre-multiplying Eq. (1) by $\mathbf{\Phi}^T$, it results in

$$\begin{aligned}&\mathbf{\Phi}^T\mathbf{M}\mathbf{\Phi}\ddot{\mathbf{q}}(t) + \mathbf{\Phi}^T\mathbf{D}\mathbf{\Phi}\dot{\mathbf{q}}(t) + \mathbf{\Phi}^T\mathbf{K}\mathbf{\Phi}\mathbf{q}(t) = \mathbf{\Phi}^T\mathbf{B_w}\mathbf{w}(t) + \mathbf{\Phi}^T\mathbf{B_u}\mathbf{u}(t) \\ &\mathbf{y}(t) = \mathbf{C_d}\mathbf{\Phi}\mathbf{q}(t) + \mathbf{C_v}\mathbf{\Phi}\dot{\mathbf{q}}(t) + \mathbf{C_w}\mathbf{w}(t) + \mathbf{C_u}\mathbf{u}(t),\end{aligned}$$

which may be written as

$$\mathbf{M_m}\ddot{\mathbf{q}}(t) + \mathbf{D_m}\dot{\mathbf{q}}(t) + \mathbf{K_m}\mathbf{q}(t) = \mathbf{B_{w_m}}\mathbf{w}(t) + \mathbf{B_{u_m}}\mathbf{u}(t) \tag{2}$$

$$\mathbf{y}(t) = \mathbf{C_{d_m}}\mathbf{q}(t) + \mathbf{C_{v_m}}\dot{\mathbf{q}}(t) + \mathbf{C_w}\mathbf{w}(t) + \mathbf{C_u}\mathbf{u}(t), \tag{3}$$

where $\mathbf{M_m} = \mathbf{\Phi}^T\mathbf{M}\mathbf{\Phi}$, $\mathbf{D_m} = \mathbf{\Phi}^T\mathbf{D}\mathbf{\Phi}$, $\mathbf{K_m} = \mathbf{\Phi}^T\mathbf{K}\mathbf{\Phi}$, $\mathbf{B_{w_m}} = \mathbf{\Phi}^T\mathbf{B_w}$, $\mathbf{B_{u_m}} = \mathbf{\Phi}^T\mathbf{B_u}$, $\mathbf{C_{d_m}} = \mathbf{C_d}\mathbf{\Phi}$, and $\mathbf{C_{v_m}} = \mathbf{C_v}\mathbf{\Phi}$. The matrices $\mathbf{M_m}$ and $\mathbf{K_m}$ are diagonal while $\mathbf{D_m}$ is not necessarily diagonal. Considering flexible structures, a reasonable assumption is $\mathbf{D} = \alpha\mathbf{M} + \beta\mathbf{K}$ for $\alpha, \beta \geq 0$ due to small damping factors (Gawronski, 2004).

For nonsingular matrix $\mathbf{M_m}$, Eq. (2) can be written as

$$\ddot{\mathbf{q}}(t) + \mathbf{M_m^{-1}}\mathbf{D_m}\dot{\mathbf{q}}(t) + \mathbf{M_m^{-1}}\mathbf{K_m}\mathbf{q}(t) = \mathbf{M_m^{-1}}\mathbf{B_{w_m}}\mathbf{w}(t) + \mathbf{M_m^{-1}}\mathbf{B_{u_m}}\mathbf{u}(t). \tag{4}$$

Adopting the state-vector definition as

$$\mathbf{x}(t) = \begin{bmatrix} \mathbf{x_1}(t) \\ \mathbf{x_2}(t) \end{bmatrix} = \begin{bmatrix} \mathbf{q}(t) \\ \dot{\mathbf{q}}(t) \end{bmatrix},$$

Eq. (3) and Eq. (4) can be transformed into

$$\begin{aligned}\dot{\mathbf{x}}_\mathbf{1}(t) &= \mathbf{x_2}(t) \\ \dot{\mathbf{x}}_\mathbf{2}(t) &= -\mathbf{M_m^{-1}}\mathbf{K_m}\mathbf{x_1}(t) - \mathbf{M_m^{-1}}\mathbf{D_m}\mathbf{x_2}(t) + \mathbf{M_m^{-1}}\mathbf{B_{w_m}}\mathbf{w}(t) + \mathbf{M_m^{-1}}\mathbf{B_{u_m}}\mathbf{u}(t) \\ \mathbf{y}(t) &= \mathbf{C_{d_m}}\mathbf{x_1}(t) + \mathbf{C_{v_m}}\mathbf{x_2}(t) + \mathbf{C_w}\mathbf{w}(t) + \mathbf{C_u}\mathbf{u}(t),\end{aligned}$$

which can be written in the state-space representation:

$$\begin{aligned}&\dot{\mathbf{x}}(t) = \mathbf{A}\mathbf{x}(t) + \mathbf{B_1}\mathbf{w}(t) + \mathbf{B_2}\mathbf{u}(t) \\ &\mathbf{y}(t) = \mathbf{C_2}\mathbf{x}(t) + \mathbf{D_{21}}\mathbf{w}(t) + \mathbf{D_{22}}\mathbf{u}(t),\end{aligned}$$

in which $\mathbf{C_2} = [\mathbf{C_{d_m}}\ \mathbf{C_{v_m}}]$, $\mathbf{D_{21}} = \mathbf{C_w}$, and $\mathbf{D_{22}} = \mathbf{C_u}$. The matrices $\mathbf{A}$, $\mathbf{B_1}$, and $\mathbf{B_2}$ are obtained as

$$\mathbf{A} = \begin{bmatrix} \mathbf{0} & \mathbf{I} \\ -\mathbf{M_m^{-1}}\mathbf{K_m} & -\mathbf{M_m^{-1}}\mathbf{D_m} \end{bmatrix},\ \mathbf{B_1} = \begin{bmatrix} \mathbf{0} \\ \mathbf{M_m^{-1}}\mathbf{B_{w_m}} \end{bmatrix},\ \text{and } \mathbf{B_2} = \begin{bmatrix} \mathbf{0} \\ \mathbf{M_m^{-1}}\mathbf{B_{u_m}} \end{bmatrix}.$$

The state-space modal model representation can be obtained applying a transformation matrix (Gawronski, 2004), which leads to the following state-space model structure adopted in this paper:

$$\bar{\mathbf{A}} = \begin{bmatrix} \mathbf{A_1} & \mathbf{0} & \cdots & \mathbf{0} \\ \mathbf{0} & \mathbf{A_2} & \cdots & \mathbf{0} \\ \vdots & \vdots & \ddots & \vdots \\ \mathbf{0} & \mathbf{0} & \cdots & \mathbf{A_m} \end{bmatrix},\ \bar{\mathbf{B}}_\mathbf{1} = \begin{bmatrix} \mathbf{B_{11}} \\ \mathbf{B_{12}} \\ \vdots \\ \mathbf{B_{1m}} \end{bmatrix},\ \bar{\mathbf{B}}_\mathbf{2} = \begin{bmatrix} \mathbf{B_{21}} \\ \mathbf{B_{22}} \\ \vdots \\ \mathbf{B_{2m}} \end{bmatrix},\ \text{and } \bar{\mathbf{C}}_\mathbf{2} = \begin{bmatrix} \mathbf{C_{21}^T} \\ \mathbf{C_{22}^T} \\ \vdots \\ \mathbf{C_{2m}^T} \end{bmatrix}^T,$$

where $\mathbf{A}_i$ is a 2×2 matrix for $i = 1 \dots m$, i.e., it isolates each mode.

3. MODAL ROBUST CONTROL

A performance vector $\mathbf{z}(t)$ is included in the modal representation to build the adopted model framework, leading to the following state-space model:

$$\begin{aligned}\dot{\mathbf{x}}(t) &= \bar{\mathbf{A}}\mathbf{x}(t) + \bar{\mathbf{B}}_\mathbf{1}\mathbf{w}(t) + \bar{\mathbf{B}}_\mathbf{2}\mathbf{u}(t)\\ \mathbf{z}(t) &= \mathbf{C_1}\mathbf{x}(t) + \mathbf{D_{11}}\mathbf{w}(t) + \mathbf{D_{12}}\mathbf{u}(t)\\ \mathbf{y}(t) &= \bar{\mathbf{C}}_\mathbf{2}\mathbf{x}(t) + \mathbf{D_{21}}\mathbf{w}(t) + \mathbf{D_{22}}\mathbf{u}(t),\end{aligned}$$

in which the matrices $\mathbf{C_1}$, $\mathbf{D_{11}}$, and $\mathbf{D_{12}}$ with appropriate dimensions are chosen to define the desired performance vector $\mathbf{z}(t)$. Considering the modal representation, the performance vector and disturbance vector $\mathbf{w}(t)$ can be decomposed into m contiguous frequency bands as $\mathbf{z}(t) = \sum_{i=1}^{m} \mathbf{z}_i(t)$ and $\mathbf{w}(t) = \sum_{i=1}^{m} \mathbf{w}_i(t)$, in which $\mathbf{z}_i(t)$ represents the performance signal relative to the distinct mode i in frequency band i (Genari *et al.*, 2017a).

Given a state-space controller K_c as

$$\begin{aligned}\dot{\mathbf{x}}_c(t) &= \mathbf{A}_c\mathbf{x}_c(t) + \mathbf{B}_c\mathbf{y}(t)\\ \mathbf{u}(t) &= \mathbf{C}_c\mathbf{x}_c(t) + \mathbf{D}_c\mathbf{y}(t),\end{aligned}$$

the modal H_∞ control problem is to compute the controller matrices such that the closed-loop system satisfies

$$\underbrace{\inf}_{K_c \in V} \; \underbrace{\sup}_{\mathbf{w} \in \mathcal{L}_2]0,\infty[} \; J_m < \gamma^2,$$

in which V represents the set of all controllers that stabilize the plant and

$$J_m = \frac{\sum_{i=1}^{m} \int_0^\infty \mathbf{z}_i^T(t)\mathbf{Q}_i\mathbf{z}_i(t)dt}{\sum_{i=1}^{m} \int_0^\infty \mathbf{w}_i^T(t)\mathbf{w}_i(t)dt}$$

is the modal H_∞ norm, in which the diagonal matrix $\mathbf{Q}_i > 0$ weights the mode i to achieve mode selectivity.

A new modal performance indicator is defined as

$$\mathbf{z_p}(t) = \mathbf{\Gamma}\mathbf{x}(t) + \mathbf{\Theta}\mathbf{w}(t) + \mathbf{\Lambda}\mathbf{u}(t),$$

which is composed by the following matrices

$$\begin{aligned}\mathbf{\Gamma} &= \left[\begin{array}{cccc} \mathbf{Q}_\mathbf{1}^{\frac{1}{2}}\mathbf{C}_{\mathbf{1_1}} & \mathbf{Q}_\mathbf{2}^{\frac{1}{2}}\mathbf{C}_{\mathbf{1_2}} & \cdots & \mathbf{Q}_\mathbf{m}^{\frac{1}{2}}\mathbf{C}_{\mathbf{1_m}} \end{array}\right],\\ \mathbf{\Theta} &= (\mathbf{Q}_\mathbf{1}^{\frac{1}{2}}\mathbf{D}_{\mathbf{11_1}} + \cdots + \mathbf{Q}_\mathbf{m}^{\frac{1}{2}}\mathbf{D}_{\mathbf{11_m}}),\\ \mathbf{\Lambda} &= (\mathbf{Q}_\mathbf{1}^{\frac{1}{2}}\mathbf{D}_{\mathbf{12_1}} + \cdots + \mathbf{Q}_\mathbf{m}^{\frac{1}{2}}\mathbf{D}_{\mathbf{12_m}}),\end{aligned}$$

in which $\mathbf{C}_{\mathbf{1}_i}$, $\mathbf{D}_{\mathbf{11}_i}$, and $\mathbf{D}_{\mathbf{12}_i}$ correspond to the respective mode i submatrices in $\mathbf{C_1}$, $\mathbf{D_{11}}$, and $\mathbf{D_{12}}$. Therefore, the modal control problem can now be solved using a known objective function (Genari *et al.*, 2017a):

$$J_\infty = \frac{\int_0^\infty \mathbf{z}_\mathbf{p}^T(t)\mathbf{z_p}(t)dt}{\int_0^\infty \mathbf{w}^T(t)\mathbf{w}(t)dt},$$

where regular techniques in H_∞ control theory can be applied to find the controller matrices.

The modal control problem is depicted in Fig. 1, including the nominal plant G_n, modal controller K_c, and weighing filters $F_\mathbf{u}$ and $F_\mathbf{z}$ whose outputs are respectively the performance vectors $\mathbf{z_u}(t)$ and $\bar{\mathbf{z}}_\mathbf{p}(t)$. These filters are used to avoid spillover, to limit the control signals, and to balance the relation between the disturbances and the performance index. Usually, $F_\mathbf{z}(s)$ is designed as a low-pass filter and $F_\mathbf{u}(s)$ is chosen as a high-pass filter (Zhou and Doyle, 1997):

$$F_\mathbf{z}(s) = \left(\frac{\frac{s}{\sqrt[k]{M}} + \omega_c}{s + \omega_c\sqrt[k]{\varepsilon}}\right)^k \text{ and } F_\mathbf{u}(s) = \left(\frac{s + \frac{\omega_c}{\sqrt[k]{M}}}{s\sqrt[k]{\varepsilon} + \omega_c}\right)^k, \tag{5}$$

in which ω_c, k, ε, and M determine the transition frequency between rejection band and passband, the filter order, the gain at passband, and the gain at the rejection band, respectively.

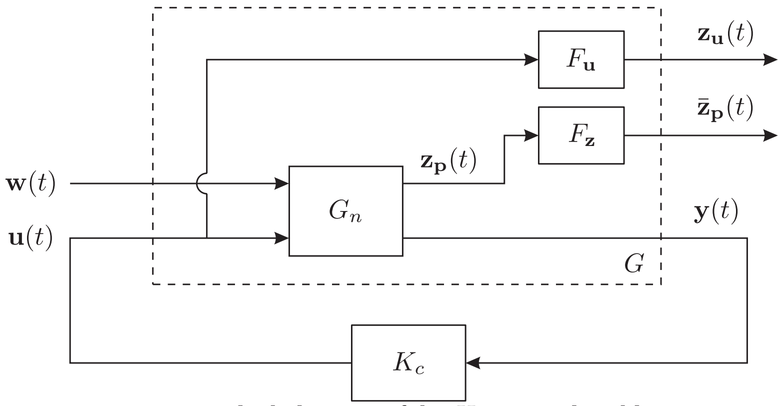

Figure 1: Block diagram of the H_∞ control problem

4. EXPERIMENTAL RESULTS

This section presents the experimental application of the modal H_∞ technique for the vibration control of a flexible structure. In the sequence, a regular H_∞ controller and some modal H_∞ controllers are designed and their performances are related to reduce structural vibration caused by disturbance.

4.1 Structure description

The flexible structure used to test the modal H_∞ methodology is a cantilever aluminum beam, shown in Fig. 2a. This structure has length of 700 mm and cross section of 3.2 mm $\times$ 32 mm. A volume equivalent to two triangular prisms were removed to amplify the vibrations caused by disturbance. Furthermore, two pairs of piezoelectric transducers (PZTs) are used to apply the disturbance and the control signal. The first PZT pair, with each PZT presenting dimensions of 0.3 mm $\times$ 20 mm $\times$ 30 mm, is placed 50 mm away from the origin and is used to apply the control signal. The second pair, with each PZT presenting dimensions of 0.2 mm $\times$ 20 mm $\times$ 30 mm is glued 120 mm far from the origin. As a sensor, only one PZT with dimensions of 0.5 mm $\times$ 20 mm $\times$ 20 mm is used to capture the vibrations 110 mm away from the end. The input signals are amplified by 20 times and are applied to their respective transducers. A dSPACE® board, model DS1104, and the ControlDesk® software are used for signal generation, data acquisition, and controller implementation. The experimental diagram is presented in Fig. 2b.

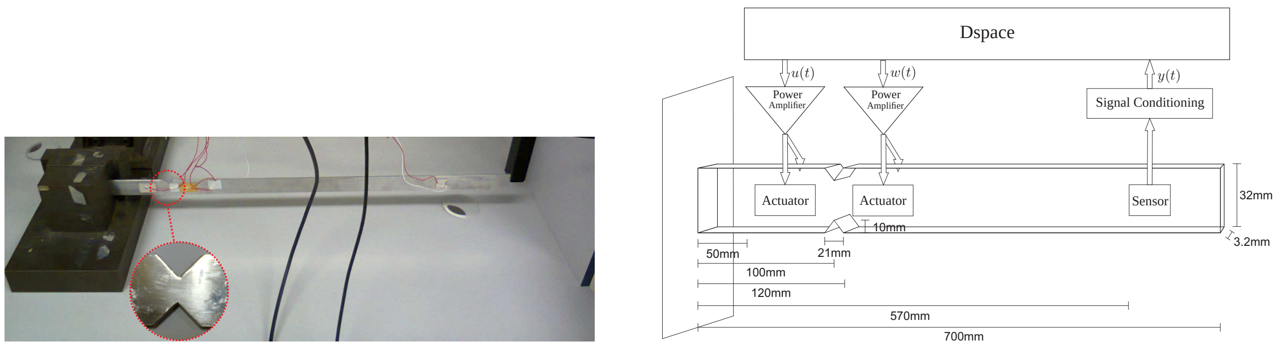

(a) Aluminum beam (b) Block diagram

Figure 2: Experiment setup

4.2 Model identification

The experimental frequency response functions (FRFs) are estimated using a Schroeder signal with bandwidth 0 Hz to 500 Hz, sampled at 4 kHz. To determinate the FRF P_{yu} between the output $y(t)$ and the control signal $u(t)$, the Schroeder signal is used as a control signal and the disturbance is set to zero. Analogously, the FRF P_{yw} between the output $y(t)$ and the disturbance signal $w(t)$ is computed using the Schroeder signal as disturbance and the control signal is set to zero. The experimental FRFs are presented in Fig. 3, in which is possible to identify six different modes. However, the two first modes in P_{yw} are much smaller than the other four modes. Furthermore, the control objective is to reduce the vibration caused by disturbance through peak vibration reduction of P_{yw}. Thus, the two first modes can be ignored for the identification, considering the control goal. The state-space modal model is identified with *ssest* function of MATLAB®, in which the identification model is compared with the experimental FRFs in Fig. 3.

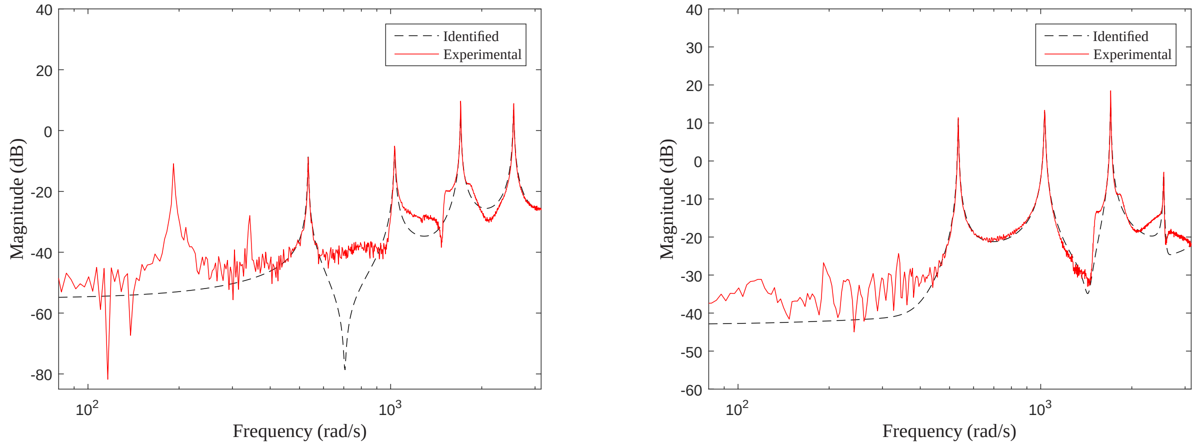

(a) P_{yu} (b) P_{yw}

Figure 3: Experimental and identified P_{yu} and P_{yw}

4.3 Modal robust controller design

The modal controller is designed using only the three first modes, in which the fourth mode is used to verify the controller effect outside of the frequency band of interest. Thus, the modal model is truncated including only the first three modes, as can be seen in Fig. 4. Furthermore, to avoid the spillover effect, the weighting filters of Eq. (5) are designed with the following parameters: $M = 255$, $k = 1$, $\varepsilon = 0.1$, and $w_c = 1800$ rad/s.

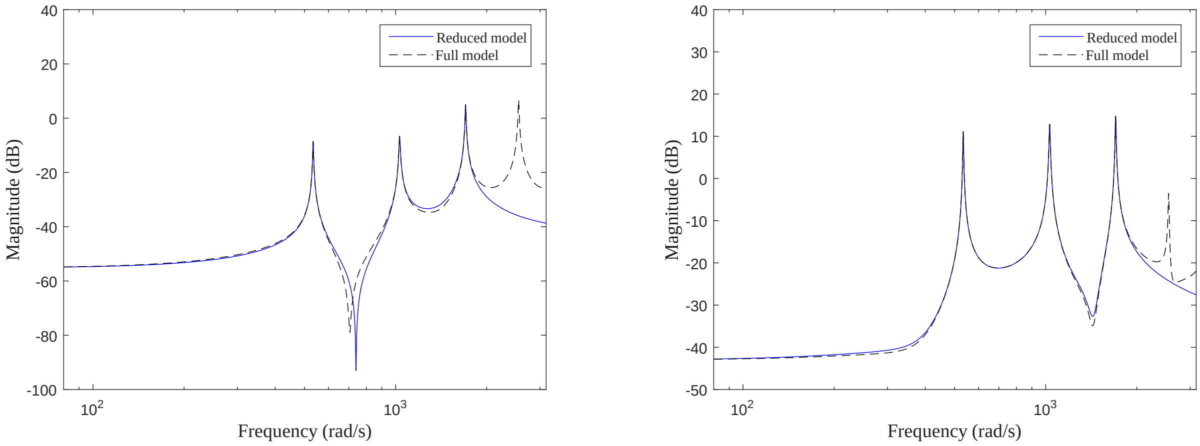

(a) Transfer functions between $y(t)$ and $u(t)$ (b) Transfer functions between $y(t)$ and $w(t)$

Figure 4: Transfer function comparison between full and reduced models

The model used to design the controller is obtained in the state-space form with matrices ($\bar{\mathbf{A}}, \bar{\mathbf{B}}_1, \bar{\mathbf{B}}_2, \bar{\mathbf{C}}_2, \mathbf{D_{21}}, \mathbf{D_{22}}$) obtained directly from the truncation of the identified model, whose performance matrices are adopted as $\bar{\mathbf{C}}_2 = \mathbf{C_1}$, $\mathbf{D_{21}} = \mathbf{D_{22}} = 0$. Moreover, the modal H_∞ problem is solved using the function *mincx* of MATLAB® and a chirp signal with band between 78 Hz and 500 Hz and amplitude of 0.5 V is considered as disturbance in the simulations and experiments to test the controllers.

The regular H_∞ controller (RC) is initially designed and its performance is used as the reference. Then, to analyse the weighting effects in the modes, three modal controllers (MC) are designed with the following weighting matrices:

1. MC1: $[\mathbf{Q_1^{\frac{1}{2}}}\ \mathbf{Q_2^{\frac{1}{2}}}\ \mathbf{Q_3^{\frac{1}{2}}}] = [0.5\ 1.0\ 1.2]$;

2. MC2: $[\mathbf{Q_1^{\frac{1}{2}}}\ \mathbf{Q_2^{\frac{1}{2}}}\ \mathbf{Q_3^{\frac{1}{2}}}] = [0.5\ 1.2\ 1.4]$;

3. MC3: $[\mathbf{Q}_1^{\frac{1}{2}}\ \mathbf{Q}_2^{\frac{1}{2}}\ \mathbf{Q}_3^{\frac{1}{2}}] = [0.5\ 1.4\ 1.6]$.

Figure 5 presents the simulated results for the maximum vibration of each mode and the control signals, where three modes are in interest bandwidth and one is outside it. For mode 1, it is possible to note that the decrease in weighing leads to modal performance loss and control signal reduction. On the other hand, the increase in weighing in modes 2 and 3 conducts to performance gain and control signal amplification. In relation to the mode 4, outside of the interest band, it is little affected by all controllers.

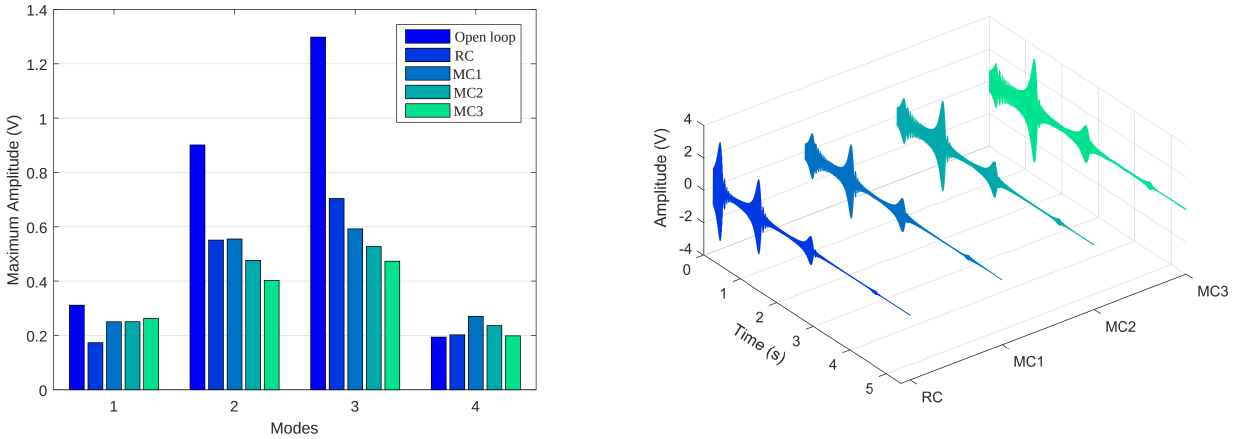

(a) Peak vibration of each mode
(b) Control signals

Figure 5: Simulated signals

4.4 Experimental application

The designed controllers are now experimentally examined in the beam. Figure 6 presents the controller performances and the control signals. One may note that the controllers have a close behavior to the simulated results, in which the modal controllers provide a superior performance in relation to regular strategy. This effectiveness is provided by an adequate modal control signal energy distribution of modal controllers, where the modal H_∞ norm is responsible to signal which modes should be prioritized. For instance, for the modes whose weights are continuously increased, their vibration amplitudes are continuously reduced. In addition, theses results show that an adequate modal vibration control is able to provide a better performance than a regular control strategy.

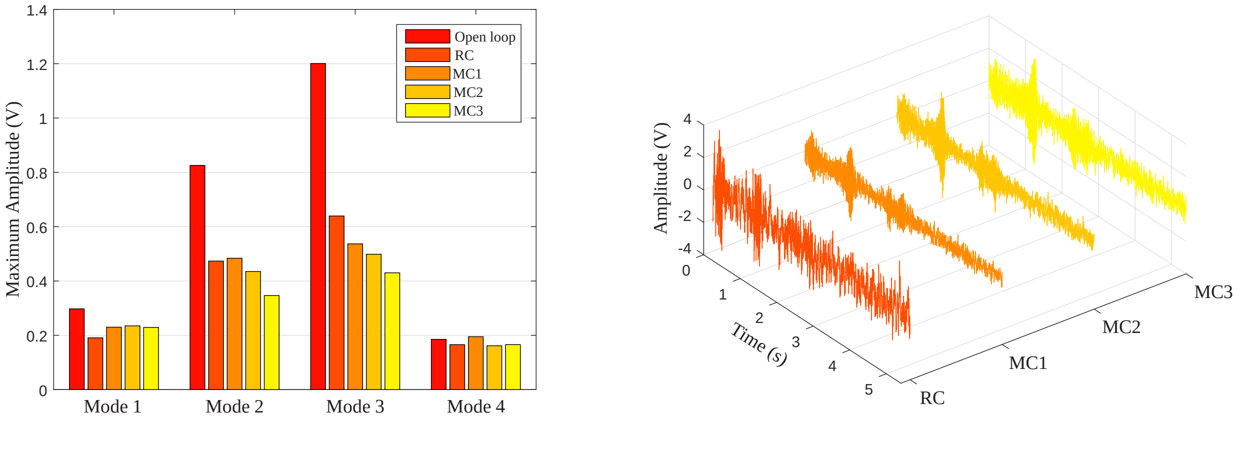

(a) Peak vibration of each mode
(b) Control signals

Figure 6: Experimental signals

5. CONCLUSIONS

This paper presents an experimental study of the new modal H_∞ control technique for structural vibration control of flexible structures. Initially, the description of a state-space modal representation is presented. Then, the modal control technique is introduced, in which the modal model characteristic is used to provide the modal H_∞ norm. Finally, experimental and simulated results show that the modal H_∞ strategy is more effective than the regular H_∞ technique in reducing structural vibration in the analyzed cases. This performance gain is due to the possibility of modal selectivity, which provides an efficient modal control energy distribution. As future work objective, more complex flexible structures will be investigated to examine the effectiveness of modal robust control for real applications. Furthermore, the proposed technique will be examined in new application areas like trajectory tracking in autonomous vehicles, polytope control problems, and fault-tolerant control.

6. ACKNOWLEDGEMENTS

The authors gratefully acknowledges the financial support received from CAPES ("PVE 2789/2014").

7. REFERENCES

Balas, M.J., 1979. "Direct velocity feedback control of large space structures". *Journal of Guidance, Control, and Dynamics*, Vol. 2, No. 3, pp. 252–253.

Baz, A. and Poh, S., 1990. "Experimental implementation of the modified independent modal space control method". *Journal of Sound and Vibration*, Vol. 139, No. 1, pp. 133–149.

Cinquemani, S., Ferrari, D. and Bayati, I., 2015. "Reduction of spillover effects on independent modal space control through optimal placement of sensors and actuators". *Smart Materials and Structures*, Vol. 24, No. 8, pp. 1–11.

Gawronski, W., 2004. *Advanced Structural Dynamics and Active Control of Structures*. Springer-Verlag.

Genari, H.F.G., Mechbal, N., Coffignal, G. and Nóbrega, E.G.O., 2017a. "Damage-tolerant active control using a modal H_∞-norm-based methodology". *Control Engineering Practice*, Vol. 60, pp. 76–86.

Genari, H.F.G., Mechbal, N., Coffignal, G. and Nóbrega, E.G.O., 2017b. "A modal H_∞-norm-based performance requirement for damage-tolerant active controller design". *Journal of Sound and Vibration*, Vol. 394, pp. 15–30.

Genari, H.F.G., Mechbal, N., Coffignal, G. and Nóbrega, E.G.O., 2017c. "A reconfigurable damage-tolerant controller based on a modal double-loop framework". *Mechanical Systems and Signal Processing*, Vol. 88, pp. 334–353.

Genari, H.F.G., Neto, O.O., Nóbrega, E.G.O., Mechbal, N. and Coffignal, G., 2015. "Robust vibration control of a vertical flexible structure subject to seismic events". In *XVII International Symposium on Dynamic Problems of Mechanics*. Natal, Brazil, pp. 1–10.

Gosiewski, Z. and Kulesza, Z., 2013. "Virtual collocation of sensors and actuators for a flexible rotor supported by active magnetic bearings". In *14th International Carpathian Control Conference*. Rytro, pp. 94–99.

Halim, D., 2004. "Control of flexible structures with spatially varying disturbance: spatial H_∞ approach". In *43rd IEEE Conference on Decision and Control*. Atlantis, Paradise Island, Bahamas, Vol. 5, pp. 5065–5070.

Hu, Y.R. and Ng, A., 2005. "Active robust vibration control of flexible structures". *Journal of Sound and Vibration*, Vol. 288, No. 1–2, pp. 43–56.

Inman, D.J., 2001. "Active modal control for smart structures". *Phil. Trans. R. Soc. Lond. A*, Vol. 359, pp. 205–219.

Mastory, C.G. and Chalhoub, N.G., 2014. "Enhanced structural controllers for non-collocated systems". *Journal of Vibration and Control*, Vol. 22, No. 3, pp. 678–694. doi:10.1177/1077546314530418.

Mechbal, N. and Nóbrega, E.G.O., 2012. "Damage tolerant active control: Concept and state of the art". In *8th IFAC Symposium on Fault Detection, Supervision and Safety of Technical Processes*. Mexico City, Mexico, pp. 63–71.

Mechbal, N. and Nóbrega, E.G.O., 2015. "Adaptive strategy to damage tolerant active control". In *9th IFAC Symposium on Fault Detection, Supervision and Safety for Technical Processes*. Paris, France, pp. 658–663.

Meirovitch, L., Baruh, H. and Oz, H., 1983. "A comparison of control techniques for large flexible systems". *Journal of Guidance, Control, and Dynamics*, Vol. 6, No. 4, pp. 302–310.

Pereira, D.A. and Serpa, A.L., 2015. "Bank of H_∞ filters for sensor fault isolation in active controlled flexible structures". *Mechanical Systems and Signal Processing*, Vol. 60-61, pp. 678–694.

Preumont, A., 2011. *Vibration Control of Active Structures: An Introduction*. Springer, 3rd edition.

Serpa, A.L. and Nobrega, E.G.O., 2005. "H_∞ Control with Pole Placement Constraints for Flexible Structures Vibration Reduction". In *18th International Congress of Mechanical Engineering*. Ouro Preto, Brazil, pp. 1–8.

Zhou, K. and Doyle, J.C., 1997. *Essentials of Robust Control*. Prentice Hall.

8. RESPONSIBILITY NOTICE

The authors are the only responsible for the printed material included in this paper.